

Characterization of the Zinc Binding Activity of the Rubella Virus Nonstructural Protease

XIN LIU,¹† JENNY YANG,² A. MOHAMAD GHAZI,³ AND TERYL K. FREY^{1*}

Departments of Biology,¹ Chemistry,² and Geology,³ Georgia State University, Atlanta, Georgia 30303

Received 22 October 1999/Accepted 13 April 2000

The rubella virus (RUB) nonstructural (NS) protein (NSP) ORF encodes a protease that cleaves the NSP precursor (240 kDa) at a single site to produce two products. A cleavage site mutation was introduced into a RUB infectious cDNA clone and found to be lethal, demonstrating that cleavage of the NSP precursor is necessary for RUB replication. Based on computer alignments, the RUB NS protease was predicted to be a papain-like cysteine protease (PCP) with the residues Cys1152 and His1273 as the catalytic dyad; however, the RUB NS protease was recently found to require divalent cations such as Zn, Co, and Cd for activity (X. Liu, S. L. Ropp, R. J. Jackson, and T. K. Frey, *J. Virol.* 72:4463–4466, 1998). To analyze the function of metal cation binding in protease activity, Zn binding studies were performed using the minimal NS protease domain within the NSP ORF. When expressed as a maltose binding protein (MBP) fusion protein by bacteria, the NS protease exhibited activity both in the bacteria and in vitro following purification when denatured and refolded in the presence of Zn. Atomic absorption analysis detected 1.6 mol of Zn bound per mol of protein refolded in this manner. Expression of individual domains within the protease as MBP fusions and analysis by a Zn⁶⁵ binding assay revealed two Zn binding domains: one located at a predicted metal binding motif beginning at Cys1175 and the other one close to the cleavage site. Mutagenesis studies showed that Cys1175 and Cys1178 in the first domain and Cys1227 and His1273, the His in the predicted catalytic site, in the second domain are essential for zinc binding. All of these residues are also necessary for the protease activity, as were several other Cys residues not involved in Zn binding. Far-UV circular dichroism (CD) analysis of the MBP-NS protease fusion protein showed that the protease domain contained a large amount of alpha-helical structure, which is consistent with the results of secondary-structural prediction. Both far-UV-CD and fluorescence studies suggested that Zn did not exert a major effect on the overall structure of the fusion protein. Finally, protease inhibitor assays found that the protease activity can be blocked by both metal ion chelators and the metalloprotease inhibitor captopril. In conjunction with the finding that the previously predicted catalytic site, His1273, is essential for zinc binding, this suggests that the RUB NS protease is actually a novel virus metalloprotease rather than a PCP.

Rubella virus (RUB) is the etiological agent of a disease known as rubella or German measles. RUB is the sole member of the *Rubivirus* genus in the *Togaviridae* family and has a positive-polarity, single-stranded RNA genome of 9,762 nucleotides (nt) which contains two long open reading frames (ORFs) (for a review, see reference 7). The 5'-proximal ORF extends from nt 41 to nt 6389 (2,116 amino acids [aa]; 240 kDa) and encodes nonstructural (NS) proteins (NSPs) primarily involved in viral RNA replication, while the 3'-proximal ORF (nt 6512 to 9700; 1,063 aa; 110 kDa) encodes the virion structural proteins. Computer-assisted comparison of the RUB NSP ORF with other plus-strand RNA viruses revealed a number of shared consensus motifs, namely, methyltransferase, protease, helicase, and replicase domains. Of these, only the protease and helicase domains have been characterized biochemically (5, 10, 19).

All of the plus-strand RNA viruses of animals thus far studied employ polyprotein processing in the expression of their replicase components. The RUB NSP ORF is first translated

into a polyprotein precursor (P200), which then undergoes proteolytic cleavage between Gly1301 and Gly1302 to produce two mature products, P150 and P90. A limited homology exists between a domain just upstream from the cleavage site and the active site of papain-like cysteine proteases (PCPs) (9). Within this domain, Cys1152 and His1273 were predicted to form the catalytic dyad and site-directed mutagenesis confirmed that both residues are essential for protease activity (5, 19). While activity was readily detected when the protease domain was expressed in vivo, activity was never observed in vitro. However, the protease was recently found to require divalent cations (Zn²⁺, Cd²⁺, or Co²⁺) for in vitro activity (18), which is a novel observation among both cellular and viral PCPs. Based on sequence analysis, there is a putative metal binding domain located within the protease domain with the sequence Cys₁₁₇₅-X₂-Cys₁₁₇₈-X₁₁-His₁₁₉₀-X₁₃-His₁₂₀₄ (6).

The goal of this study was to determine whether the RUB NS protease binds zinc and to analyze the role that zinc plays in enzyme activity. Metal ions such as zinc have been shown to play both structural and catalytic roles in proteases; however, no true viral metalloproteases have been discovered although viral proteases which require zinc for activity have been described. For two viral Zn binding proteases whose structures have been studied, the hepatitis C virus (HCV) NS2-3 protease and the human rhinovirus (HRV) 2A protease, Zn was found to play a structural role (16, 25, 26, 32).

* Corresponding author. Mailing address: Department of Biology, Georgia State University, Atlanta, GA 30303. Phone: (404) 651-3105. Fax: (404) 651-3105. E-mail: tfrey@gsu.edu.

† Present address: Measles Section, Division of Viral and Rickettsial Diseases, U.S. Centers for Disease Control and Prevention, Atlanta, GA 30333.

TABLE 1. Oligonucleotide primers used for cloning in pMAL-c2

Construct ^a	Primer pair (upstream + downstream)
RP1	1 (CGCGAATTCGGTGACCCGGGCCGA) + 2 (CGCAAGCTTACCGCCCCGAGACAG)
RP2	1 + 3 (CGCAAGCTTAGACCTGGCGGCCGTC)
ZPa	1 + 4 (CGCAAGCTTATCCGGTGCCGTCAGG)
ZPb	5 (CGCGAATTCGGCGGCGAGCTAGAC) + 3
ZP1	1 + 6 (CGCAAGCTTATCCGGTGCTCGCCCG)
ZP2	5 + 4
ZP3	7 (CGCGAATTCGGAGATCCCCTCGAC) + 3

^a Regions of the NSP ORF (Fig. 1) were PCR amplified from the template Robo302 or pTM1/nsRUB* using the primer pairs shown for insertion into pMAL-c2. In each primer, the restriction site used for cloning is underlined and the in-frame stop codon is in boldface in the downstream primer.

MATERIALS AND METHODS

Plasmid constructions and site-directed mutagenesis. Plasmids pTM1/nsRUB and pTM1/nsRUB*, in which transcription and translation of the RUB NSP ORF are under control of the T7 polymerase promoter and the internal ribosome entry site of encephalomyocarditis virus, respectively, as well as Robo302, a RUB infectious cDNA clone, were described previously (18, 19, 20). pTM1/nsRUB* contains a Cys1152Gly mutation which abrogates NS protease activity. pTM1/nsSIN123, a construct corresponding to pTM1/nsRUB which contains the nsP1-nsP2-nsP3 region of the Sindbis virus NSP ORF with an active nsP2 protein, was obtained from Charles Rice. The fusion protein expression system pMAL-c2 (New England Biolabs) was used to express regions of the RUB NSP ORF as maltose binding protein (MBP) fusion proteins. These regions were amplified by PCR from Robo302 with the primer pairs shown in Table 1. The 5' member of each pair contained an *Eco*RI restriction site for insertion of the amino acid coding sequence in frame with the MBP sequence, while the 3' member contained a *Hind*III restriction site to allow directional insertion. Constructs containing the Cys1152Gly mutation were amplified from pTM1/nsRUB*. Site-directed mutagenesis was done with complementary primers each containing the mutation (13); the primers used for each mutation are shown in Table 2. First-round PCR was done using each mutagenic primer and an outside primer to produce a fragment encompassing a convenient restriction site. Second-round PCR using the two outside primers and the first-round fragment produced a mutagenized fragment which was inserted into pTM1/nsRUB or a pMAL-c2 construct. PCR amplification using *ExTaq* polymerase (TaKaRa LA PCR Kit; Pan Vera Corp., Madison, Wis.) and subsequent cloning were done as previously described (20). Sequencing of each construct and mutation were done to make sure that the NSP region was in frame and that the mutations were as intended.

Fusion protein expression and purification. Exponential cultures of *Escherichia coli* DH5 α containing pMAL-c2 constructs were induced with 0.8 mM isopropyl- β -D-thiogalactopyranoside (IPTG) for 2.5 h. After collection by centrifugation, the cell pellet was suspended in column buffer (10 mM Tris-HCl, 1 mM EDTA, pH 8.0) and passed twice through a French press (SLM Instruments, Inc.) at a cell pressure of 10,000 lb/in². The cell lysate was centrifuged at 20,000 rpm, and the supernatant was used as the source of fusion protein, which was initially purified by affinity chromatography on amylose resin (New England Biolabs); elution was with 10 mM maltose. For protease activity assays and atomic absorption analysis, further purification was performed using fast-performance liquid chromatography. Proteins eluted from amylose columns were loaded onto a Mono Q column (Pharmacia) and further eluted with a buffer gradient of 25 to 500 mM NaCl in 20 mM Tris-HCl (pH 7.4) at a column speed of 0.5 ml/min. Fractions were monitored by determination of A_{280} or by sodium dodecyl sulfate (SDS)-polyacrylamide gel electrophoresis (PAGE); the fusion proteins were usually eluted at 250 mM NaCl.

In vitro reconstitution of expressed protease activity. Purified fusion proteins containing the complete protease domain (RP2 and RP2*) were denatured in 6 M urea-10 mM HEPES (pH 7.5)-150 mM NaCl-10 mM dithiothreitol

(DTT)-50 mM 2-mercaptoethanol at room temperature for 2 h (22). Renaturation was initiated by rapid dilution into a 50-fold excess of buffer containing 10 mM HEPES (pH 7.5), 150 mM NaCl, 10 mM DTT, 50 mM 2-mercaptoethanol, and 0.1 mM ZnCl₂ and incubation on ice for 2 h. The refolded sample was then dialyzed overnight against two changes of 200 volumes of buffer (10 mM HEPES [pH 7.5], 100 mM NaCl, 0.1 mM ZnCl₂) at 4°C. The dialyzed fusion protein was concentrated using a Centriprep 30 concentrator (Amicon) to a final volume of 1 ml, and the concentrated protein solution was clarified by centrifugation. To detect activity, aliquots of the supernatant were added directly to the *trans*-cleavage assay described below.

Atomic absorption analysis. Aliquots of purified RP2 fusion protein denatured and renatured in the presence of 100 μ M ZnCl₂ or 5 mM EDTA as already described were then dialyzed against 500 ml of 20 mM Tris · HCl (pH 7.4)-20 mM NaCl at 4°C for 4 days with daily buffer changes to eliminate excess metal ions or chelators. Chelex-100 resin (Bio-Rad) was used to remove trace metal ions in all buffers. RP2 concentrations were determined spectrophotometrically using an extinction coefficient at an optical density at 280 nm of 6.22 mg/ml · cm. This extinction coefficient was determined by amino acid analysis carried out at the Centers for Disease Control and Prevention. Alcohol dehydrogenase (purchased from Sigma), a known zinc binding protein with two Zn sites, was used as a positive control. The specimens were analyzed by laser ablation-inductively coupled plasma mass spectroscopy. The dialyzed buffer after Chelex treatment was used as a blank, and the residual Zn background of 20 ppm was subtracted from the measurement of protein samples.

Zinc binding assay. Exponential cultures of *E. coli* containing pMAL-C2 constructs were induced with IPTG for 2.5 h and then collected by centrifugation, lysed in sample buffer (50 mM Tris-HCl [pH 6.8], 100 mM DTT, 2% SDS, 0.1% bromophenol blue, 10% glycerol), heated at 100°C for 3 min, and then resolved by SDS-10% PAGE on a duplicate set of gels. One of the gels was stained with Coomassie blue, and the contents of the other gel were transferred to a nitrocellulose membrane (Schleicher & Schuell, Keene, N.H.) using a Bio-Rad Trans-Blot cell. The membrane was first incubated in renaturing buffer (100 mM Tris-HCl [pH 6.8], 50 mM NaCl, 10 mM DTT) for 1 h with three changes of buffer (it has been shown that buffers at pH 6.8 can increase the level of stringency for zinc binding (4)). The blot was then rinsed in labeling buffer (100 mM Tris-HCl [pH 6.8], 50 mM NaCl), which was flushed with N₂ to remove dissolved oxygen to avoid oxidation of blotted proteins. After incubation with 80 μ Ci of ⁶⁵ZnCl₂ (Amersham; 0.1 mCi/mg of Zn) in 20 ml of labeling buffer for 30 min, the filter was rinsed twice in washing buffer (100 mM Tris-HCl [pH 6.8], 50 mM NaCl, 1 mM DTT) and then washed for 1 h against three changes of washing buffer. Zinc binding was detected by exposure to XAR film (Kodak).

Coupled transcription-translation assay. pTM1/nsRUB constructs and pTM3/nsSIN123 were used to program TNT Coupled Transcription/Translation System (Promega) reactions in accordance with the manufacturer's instructions, except that 100 μ M ZnCl₂ was added (18). All plasmids added to the reaction mixtures were purified by CsCl₂ equilibrium centrifugation or with a Qiagen plasmid purification kit (QIAGEN Inc.). Trans³⁵S-label (1,175 Ci/mmol; ICN) was added

TABLE 2. Oligonucleotide primers used for site-directed mutagenesis

Mutation ^a	Complementary primer pair (forward + reverse)
Cys1167Ser	8 (GCGCGCCGCTCCGGCGCC) + 9 (GCGCCGGAGGCGGCGCGC)
Cys1175Ser	10 (AGTGCCGGGTCCCCAAG) + 11 (CTTGGGGACCCGGCACT)
Cys1178Ser	12 (TGCCCAAGTCCGCTAC) + 13 (GTAGGCCAGACTGGGGCA)
His1190Leu	14 (GCCGCACTCTTGAGGAC) + 15 (GTCCTCAAGAGTGC GGCC)
His1204Leu	16 (GTGTCCCTTCTCCGTGCC) + 17 (GCACCGAGAAGGGACAC)
Cys1225Ser	18 (ACCGTGGGATCCACCTGT) + 19 (ACAGGTGGATCCCACGGT)
Cys1227Ser	20 (GGATGCACCTTCTCGCGC) + 21 (GCGCGAAGAGGTGCATCC)
His1236Leu	22 (GGCTCCGAGCTTGAGGCC) + 23 (GGCCTCAAGCTCGGAGCC)

^a Site-directed mutagenesis was initiated with complementary primers, each containing the intended mutation (underlined). Cys (TGC or TGT) was mutated to Ser (TCC or TCT), and His (CAC or CAT) was mutated to Leu (CTT or CTC) by single-base substitution.

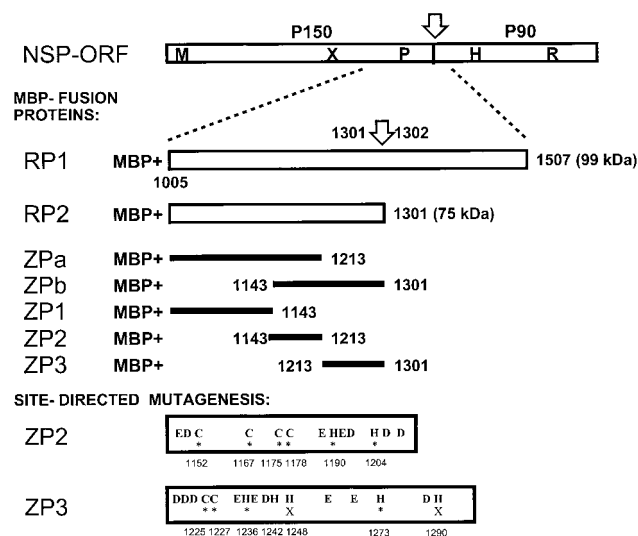


FIG. 1. Fusion protein constructs and site-directed mutagenesis of the NS protease domain. A schematic diagram of the RUB NSP ORF is shown at the top. The locations of amino acid motifs indicative of methyltransferase (M), protease (P), helicase (H), and replicase (R) are shown. X is a motif with an unknown function found in togaviruses and coronaviruses (9). The regions expressed as bacterial MBP fusion proteins are diagrammed in expanded form. Potential Zn binding ligands (Asp, Cys, Glu, and His) are indicated at the bottom. Cys and His residues mutagenized in this study are marked by asterisks, and the residue numbers are given. His residues found in an earlier study (5) not to be required for protease activity are marked by an X.

to the reaction mixture to radiolabel the translated products, which were subsequently resolved by SDS-10% PAGE. For *trans*-cleavage assays, pTM1/nsRUB*, which fails to cleave and thus produces only the P200 precursor, was used to program a standard TNT reaction. Following completion of the reaction, reconstituted fusion proteins were added directly to the reaction mixture and after incubation at 30°C for 120 min, cleavage was assayed by SDS-PAGE.

To test the effect of protease inhibitors on NS protease-mediated cleavage of P200, a variety of proteinase inhibitors were added directly to TNT reaction mixtures programmed with pTM1/nsRUB, including antipain hydrochloride (0.2 mg/ml), DTT (10 mM), E-64 or E-64C (2 mg/ml), EGTA (1 mM), phenylmethylsulfonyl fluoride (PMSF; 2 mM), tosyl lysyl chloromethyl ketone (TLCK; 0.1 mg/ml), thiorphan (1 mM), phosphoramidon (1 mM), and captopril (2 mM). To test whether chelators and alkylating agents can inhibit the transcription-translation process, reaction mixtures programmed with pTM1/nsRUB were incubated for 40 min to allow synthesis of the P200 precursor and then final concentrations of cycloheximide at 1 mg/ml, RNase A at 1 mg/ml, and 1 mM nonradiolabeled methionine were added to prevent further translation (18). The following inhibitors were then added one at a time, followed by incubation for an additional 120 min: EDTA (1 mM), 1,10-phenanthroline (1,10-OP; 1 mM), *N*-ethylmaleimide (5 mM), and iodoacetamide (5 mM).

Conformational analyses. Far-UV circular dichroism (CD) measurements were carried out using a Jasco J-710 Spectropolarimeter. RP2 fusion protein was denatured, renatured in the presence of zinc or EDTA, and then adjusted to a final concentration of 1.6 μ M in 20 mM Tris · HCl (pH 7.4). CD measurements were performed at room temperature using a 1-mm cell at 0.5-nm intervals over a wavelength range of 200 to 260 nm. All spectra were averages of eight scans with a scan rate of 50 nm/min. Mean residue molar ellipticities [θ] (degrees per square centimeter per decimole) are reported. Fluorescence experiments were performed using a PTI lifetime fluorimeter equipped with a fluorescence cell with a 1-cm path length. The protein concentration was adjusted to 0.5 μ M in 20 mM Tris-HCl buffer at pH 7.4. The emission scan wavelength was 300 to 400 nm, while the maximal excitation wavelength was \sim 280 nm.

In vitro transcription and transfection of Vero cell. To make protease mutations in the RUB infectious cDNA clone Robo302, the *RsrII-EcoRV* fragment from pTM1/nsRUB JV (cleavage site G1301 mutated to Val) (18) was transferred to Robo302, the RUB infectious clone. Sequencing was performed to make sure that the mutation was successfully introduced. Mutated Robo302 plasmids were linearized by *EcoRI* and transcribed in vitro with SP6 RNA polymerase (Epicentre Technologies) in the presence of an m7G(5')ppp(5')G cap analog, and the resulting transcripts were used to transfect Vero cells as previously described (20).

RESULTS

Expression of the RUB NS protease as a bacterial fusion protein. Two regions of the RUB NSP ORF containing the NS protease were introduced into the pMAL-c2 vector and over-expressed in *E. coli* as MBP fusion proteins. RP1 (aa 1005 to 1507 of the NSP ORF; Fig. 1) contained both the protease domain and the cleavage site and was shown to be active when expressed *in vivo* in a previous study (5), while RP2 (aa 1005 to 1301) terminated at the cleavage site. Two mutants, RP1* and RP2*, which contain the catalytic site Cys1152-Gly mutation were similarly expressed. As shown in Fig. 2a, a protein of 75 kDa was produced by RP2 while proteins of 99 and 75 kDa were produced by RP1. These (75 and 99 kDa) were the predicted sizes of the RP2 and RP1 fusion proteins, respectively. If the NS protease were active within the fusion construct, autocatalysis by RP1 would lead to production of a product the size of RP2, as was observed. No 75-kDa product was produced by catalytic-site mutant protein RP1* (Fig. 2A, lane 1), confirming that production of the 75-kDa species by RP1 was due to the NS protease. Thus, the RUB NS protease fusion protein retained its activity in the bacteria.

The expression vector pMal-C2 contains a factor Xa cleavage site between MBP and the partner protein; however, we found Xa factor cleavage of the RP1 and RP2 fusions to be low in efficiency, with nonspecific cleavage being evident, and thus, attempts to isolate the NS protease by itself were fruitless. Since the RP fusion protein exhibited protease activity in *E. coli*, experiments were done to determine if the purified fusion proteins retained activity. As a target, pTM1/nsRUB*, which lacks protease activity, was translated *in vitro* in the presence of [³⁵S]methionine and the P200 product was then exposed to RP2 or RP2*; however, no activity was observed (data not shown). Reasoning that these proteins had possibly lost their correct conformation during the purification process, we denatured purified RP2 and RP2* in 6 M urea and renatured them in the presence of 100 μ M ZnCl₂. As shown in Fig. 2B, the P200 target was processed by refolded RP2 but was not cleaved by RP2*. Thus, the activity of the MBP-NS protease

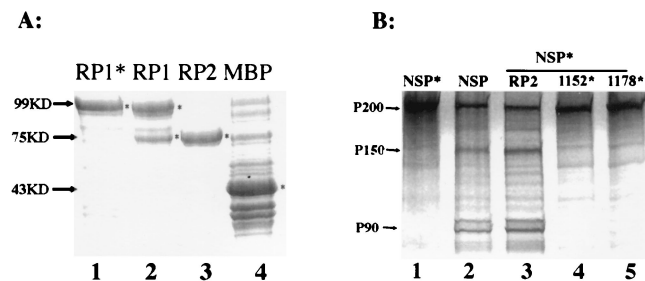


FIG. 2. Activity of NS protease expressed as a bacterial fusion protein. (A) *In vivo* activity in bacteria. Domains of the RUB NSP ORF were expressed in *E. coli* as MBP fusions. Construct RP1 contained aa 1005 to 1507 (the cleavage site is at aa 1301), and RP2 contained aa 1005 to 1301. RP1* was similar to RP1 but contained a Cys1152Gly mutation that inactivates the protease. Following expression, total bacterial lysates were chromatographed on amylose resin and the eluted proteins were resolved by SDS-PAGE followed by Coomassie blue staining. Lanes: 1, RP1*; 2, RP1; 3, RP2; 4, MBP. The expected sizes of the RP1, RP2, and MBP products are 99, 75, and 43 kDa, respectively, and are marked by asterisks. (B) *In vitro trans*-cleavage assay. pTM1/nsRUB* (lane 1) or pTM1/nsRUB (lane 2) DNA was used to program a coupled transcription-translation reaction in the presence of radiolabel. The pTM1/nsRUB* product was then incubated with purified RP2 fusion protein that was denatured and then refolded in the presence of 100 μ M ZnCl₂ (lane 3). The assay was also done with two similarly treated RP2 fusion proteins containing the mutation (indicated by asterisks) Cys1152Gly (lane 4) or Cys1178Ser (lane 5).

TABLE 3. Analysis of zinc content by atomic absorption spectroscopy

Sample ^a	Protein concn (μM)	Avg Zn content (ppb) ± SD ^b	Zn/protein molar ratio
RP2	1.4	93 ± 0.4	1.0
RP2 + ZnCl ₂	1.4	145 ± 1.0	1.6
RP2 + ZnCl ₂	2.0	204 ± 0.5	1.6
RP2 + EDTA	1.3	0	0
Alcohol dehydrogenase	1.0	121 ± 0.4	1.9

^a Purified RP2 and alcohol dehydrogenase were dissolved in water and dialyzed against 20 mM Tris (pH 7.4)–20 mM NaCl overnight. Purified RP2 was denatured in 6 M urea, renatured in buffer containing 100 μM ZnCl₂ or 1 mM EDTA, and then dialyzed against 20 mM NaCl–20 mM Tris (pH 7.4) for 4 days. Two preparations of RP2 dialyzed against Zn were analyzed.

^b Two or three analyses were done on each preparation.

fusion was recoverable by refolding and the refolded product could be considered an active enzyme for structural studies.

Zinc binding studies and Zn binding domain mapping. Metal binding was initially approached by atomic absorption spectrometry to quantitate the amount of zinc bound by the fusion protein RP2, since MBP itself does not bind zinc (8, 11). Horse liver alcohol dehydrogenase (purchased as a purified protein), which binds two zinc atoms per enzyme molecule (29), was used as a positive control. The enzyme was dissolved in water and dialyzed against zinc-free buffer (20 mM Tris, 20 mM NaCl) overnight. We detected 1.9 mol of zinc per mol of alcohol dehydrogenase (Table 3), which agrees well with the literature data. As shown in Table 3, purified RP2, after dialysis against Zn-free buffer, was found to bind 1 mol of Zn/mol of protein. When the purified protein was denatured in urea, renatured in the presence of EDTA, and then then dialyzed against Zn-free buffer for 4 days, no Zn was found in the protein sample. When renaturation was done in the presence of ZnCl₂, the zinc content was 1.6 mol/mol of protein. These data indicate that there are two metal binding sites with different affinities, with Zn being lost from the low-affinity site during purification. Both zinc ions could be chelated and removed by the chelator EDTA.

To localize the Zn binding domain within the RUB NS protease, a standard zinc binding assay was employed (4). MBP fusion proteins were blotted onto nitrocellulose following SDS-PAGE and then allowed to renature in the presence of ⁶⁵Zn. Initially, RP2, as well as the positive control alcohol dehydrogenase and the negative control MBP, was tested. Alcohol dehydrogenase and RP2 were shown to bind Zn (Fig. 3A, lane 6), while MBP alone did not show any Zn binding activity (Fig. 3A, lane 5). These data support the results of our atomic absorption studies showing that the RUB NS protease domain RP2 contains zinc binding sites. Since residues Cys1175, Cys1178, His1190, and His1204 in the RP2 domain were previously predicted to be Zn binding residues (6), mutant RP2 proteins with single mutations of each of these predicted residues were tested; however, all of these RP2 proteins with single mutations were able to bind zinc (data not shown). Although this result could indicate that none of these residues is essential for Zn binding, it is more likely that the single-site mutations would not eliminate the two zinc binding sites identified by atomic absorption studies. MBP fusion constructs were thus designed to subdivide RP2 into ZPa (aa 1005 to 1213) and ZPb (aa 1143 to 1301), as shown in Fig. 1. As shown in Fig. 3A, both ZPa and ZPb were able to bind zinc and thus, RP2 was further subdivided into three nonoverlapping regions, ZP1 (RUB aa 1005 to 1143), ZP2 (RUB aa 1143 to 1213), and ZP3 (RUB aa 1213 to 1301). As shown in Fig. 3B, both ZP2

and ZP3 bound zinc while ZP1 did not, thus demonstrating the presence of two Zn binding sites.

Cys and His residues are the most common amino acid residues involved in zinc binding (31). Mutagenesis of Cys and His residues within the ZP2 and ZP3 domains (Fig. 1) was performed to identify the amino acids essential for zinc binding. ZP2 contained four Cys (positions 1152, 1167, 1175, and 1178) and two His (positions 1190 and 1204) residues, of which Cys1175, Cys1178, His1190, and His1204 were previously predicted to constitute a Zn binding motif (6). As shown in Fig. 3C, zinc binding was detected with unmutated ZP2 (lane 1) and four proteins with single-site mutations, Cys1152Gly (lane 2), Cys1167Ser (lane 3), His1190Leu (lane 6), and His1204Leu (lane 7). In contrast, zinc binding was substantially reduced with the Cys1175Ser or Cys1178Ser mutant protein. It has been the experience in other mutational studies of zinc binding proteins that, in a ⁶⁵Zn binding assay, some residual binding to proteins in which the Zn binding site has been mutated occurs (4, 14). These data indicate that Cys1175 and Cys1178 are essential for zinc binding, agreeing with the Zn motif prediction. On the other hand, His1190 and His1204 were not essential for zinc binding although they were predicted to be zinc binding residues. Cys1152 was previously reported to be important for the protease activity (5, 19); however, Cys1152,

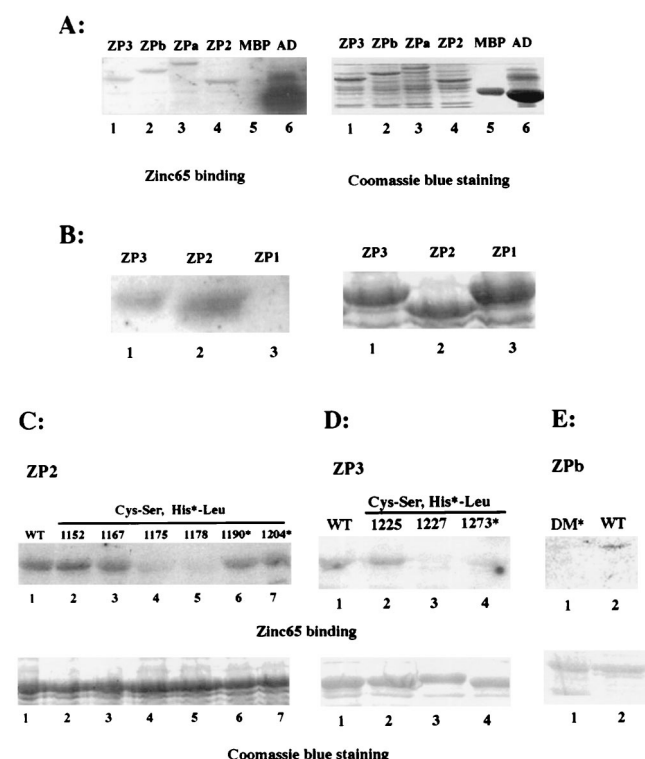


FIG. 3. Zinc binding studies. Different motifs within the RUB NS protease domain were expressed as MBP fusion proteins and resolved by SDS-PAGE on a pair of gels. The contents of one gel were transferred to a nitrocellulose membrane and then incubated with ⁶⁵ZnCl₂; the other one was stained with Coomassie blue to visualize the proteins and compare the relative concentrations. (A) Lanes: 1, ZP3; 2, ZPb; 3, ZPa; 4, ZP2; 5, MBP; 6, alcohol dehydrogenase. (B) Lanes: 1, ZP3; 2, ZP2; 3, ZP1. (C) ZP2 (lane 1) or ZP2 containing the following mutation: lane 2, Cys1152Gly; lane 3, Cys1167Ser; lane 4, Cys1175Ser; lane 5, Cys1178Ser; lane 6, His1190Leu; lane 7, His1204Leu. (D) ZP3 (lane 1) or ZP3 containing the following mutation: lane 2, Cys1225Ser; lane 3, Cys1227Ser; lane 4, His1273Leu. (E) Lanes: 1, ZPb containing the mutations Cys1178Ser and Cys1227Ser (DM*); 2, ZPb (wild type [WT]).

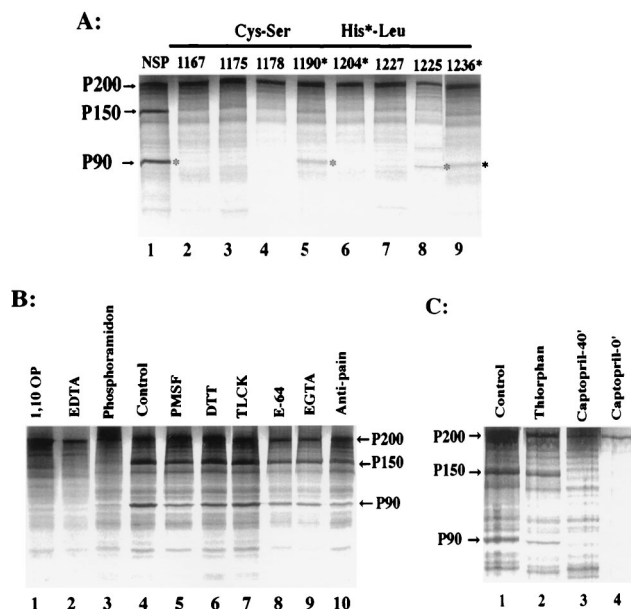


FIG. 4. Protease activity assays. (A) pTM1/nsRUB or one of its derivatives was used to program a coupled transcription-translation system. The reaction was allowed to proceed for 2 h and followed by analysis by SDS-PAGE. Lanes: 1, pTM1/nsRUB; 2, pTM1/nsRUB with Cys1167Ser; 3, Cys1175Ser; 4, Cys1178Ser; 5, His1190Leu; 6, His1204Leu; 7, Cys1227Ser; 8, Cys1225Ser; 9, His1236Leu. Cleavage is best observed in this gel by the generation of P90, whose presence is indicated by an asterisk. (B and C) Protease inhibitor assays. Coupled transcription-translation reactions were programmed with pTM1/nsRUB in the presence of one of the following protease inhibitors: B, lane 3, phosphoramidon (1 mM); B, lane 4, no inhibitor added; B, lane 5, PMSF (1 mM); B, lane 6, DTT (1 mM); B, lane 7, TLCK (10 μ g/ml); B, lane 8, E-64 (2 mM); B, lane 9, EGTA (5 mM); B, lane 10, antipain (50 μ g/ml); C, lane 4, captopril (1 mM). Where the presence of metal chelators would inhibit transcription-translation, the reaction mixture was incubated at 30°C for 40 min and RNase and cycloheximide were added to stop further translation. The inhibitors were then added to the reaction mixture, and incubation was continued for another 120 min. (B) Lanes: 1, 1,10-OP (1 mM); 2, EDTA (1 mM). (C) Lanes: 1, no inhibitor added; 2, thiorphan (1 mM); 3, captopril (1 mM).

along with Cys1167, His1190, and His1204, was not essential for zinc binding.

While ZP3 does not contain a classic Zn binding motif, it does contain a number of Cys and His residues. The data in Fig. 3D reveal that the Cys1225Ser mutation did not reduce zinc binding but Zn binding ability was substantially reduced in both the Cys1227Ser and His1273Leu mutant proteins, suggesting that Cys1227 and His1273 in ZP3 are crucial for zinc binding. A double mutation made at both Cys1178 and Cys1227 in RP2 eliminated zinc binding activity (Fig. 3E), indicating that the RUB NS protease region has two zinc binding domains that are encoded into two sequence regions, ZP2 and ZP3, and that a third zinc binding region was not missed by splitting when the protein was subdivided.

Correlation of zinc binding with protease activity. All of the site-specific mutations of Cys and His residues made as described above were transferred individually into pTM1/nsRUB, and each construct was used to program a coupled transcription-translation reaction to determine the effect of the mutation on cleavage of the P200 precursor. Figure 4A and Table 4 show that the Cys1167Ser, Cys1175Ser, Cys1178Ser, His1204Leu, and Cys1227Ser mutations resulted in complete abolition of cleavage. In addition, it has previously been shown that Cys1152 and His1273 are also essential amino acids for protease function (5, 19). Mutation of four of these, Cys1175, Cys1178, Cys1227, and His1273, inhibited zinc binding. In contrast, the

mutations His1190Leu, Cys1225Ser, and His1236Leu neither abolished zinc binding nor affected protease activity. Thus, the protease activity profile of these mutations correlated well with the zinc binding profile, indicating that the amino acids critical for zinc binding are required for activity of the protease.

Protease inhibitor assays. To further characterize the function of Zn in NS protease activity, the effect of a battery of protease inhibitors was studied. Several of these inhibitors which have no effect on translation or acquisition of protein conformation following translation were added directly to coupled transcription-translation reaction mixtures programmed with pTM1/nsRUB at the beginning of the reaction. Other inhibitors, such as metal chelators and alkylating agents which have effects on both translation and acquisition of conformation, were added after 40 min, the time required for synthesis of the P200 precursor but before significant processing is detected (17). The results are shown in Fig. 4B and C. Two serine protease inhibitors (PMSF and TLCK; Fig. 4B, lanes 5 and 7) and two cysteine protease inhibitors (E-64 and antipain; Fig. 4B, lanes 8 and 10) (12) failed to prevent the RUB NS protease from processing. This latter result was surprising considering that the NS protease is a putative PCP. However, these cysteine protease inhibitors also did not inhibit the SIN nsP2 protease when an analogous SIN NSP ORF construct, pTM3/nsSIN123, was tested similarly (data not shown), indicating that these inhibitors are not active against viral PCPs in vitro. DTT exhibited no inhibition (lane B6), indicating that disulfide bonds are not essential for protease activity. Of the metal chelators tested, EDTA and 1,10-OP (both of which were added at 40 min; Fig. 4B, lanes 1 and 2) inhibited the protease activity while EGTA (present from the beginning of the reaction; Fig. 4B, lane 9) did not. Interestingly, captopril, which is known to inhibit angiotensin-converting enzyme, which contains two zinc-dependent catalytic domains (1) inhibited the RUB NS protease activity (Fig. 4C, lanes 3 and 4). Two other metalloprotease inhibitors, thiorphan, a metalloprotease inhibitor which can inhibit neutral endopeptidase, and phosphoramidon, a bacterial metalloprotease and thermolysin inhibitor (16), appeared to exhibit some inhibition (Fig. 4B, lane 3, and C, lane 2); inhibition by phosphoramidon was greater than that

TABLE 4. Mutagenesis of Cys and His residues in NS protease

Region and residue ^a	Zn binding	Protease activity
ZP2		
Cys1152	+	- ^b
Cys1167	+	-
Cys1175	-	-
Cys1178	-	-
His1190	+	+
His1204	+	-
ZP3		
Cys1225	+	+
Cys1227	-	-
His1236	ND ^c	+
His1242	ND	ND
His1248	ND	+ ^b
His 1273	-	- ^b
His1290	ND	+ ^b

^a All of the Cys and His residues within the ZP2 and ZP3 regions of the NS protease are listed. These residues were individually mutated to determine the effect of each mutation on the retention (+) or abrogation (-) of Zn binding and protease activity.

^b Testing of the effect of mutation of this residue on protease activity was done in a previous study (5).

^c ND, not done.

by thirophan. However, neither of these inhibitors inhibited cleavage completely, as did captopril. No inhibition of the SIN nsP2 protease was observed in the presence of EDTA, 1,10-OP, or captopril (data not shown).

Conformational analyses. When aa residues 1005 to 1301 of the NSP (the sequence present in RP2) were subjected to secondary-structure prediction analysis by PHD (21), RP2 was found to have the $\alpha + \beta$ structural organization. Residues 1038 to 1045 and 1065 to 1074 (in ZP1) near the N terminus and residues 1218 to 1223, 1227 to 1232, 1256 to 1262, 1273 to 1276, and 1292 to 1296 (in ZP3) in the C-terminal third were predicted to have a beta-sheet structure. Interestingly, two crucial zinc binding residues, Cys1227 and His1273, in the ZP3 fragment were located at the beginning of beta strands. ZP2 was predicted to have a predominately alpha-helical conformation, in which residues 1151 to 1167, 1182 to 1189, and 1189 to 1197 have a strong helical propensity. Two crucial zinc binding residues, C1175 and C1178, were located in an unstructured region with large solvent accessibility. The computer program BLAST was further applied for primary sequence alignment (2). Interestingly, relatively high local homology between the Cys1175-to-Cys1178 binding pocket of ZP2 and that of the partial metal binding sites of eight different types of the metallothionein in the SwissProt database was observed (Fig. 5A) (27).

Far-UV CD analysis and fluorescence spectrum analysis were carried out to confirm these predictions and to determine if Zn binding results in a significant change in the overall structure of the protease domain. Purified MBP-RP2 was denatured and refolded in the presence of 100 μ M ZnCl₂ or 1 mM EDTA; the results of the CD analysis are shown in Fig. 5B. The wavelengths measured for far-UV CD were 200 to 260 nm at pH 7.4. In the presence of Zn, the far-UV CD spectrum of MBP-RP2 had two negative maxima at 208 and 222 nm, which is a characteristic of helical conformation. The mean residue ellipticity at 222 nm for RP2 was about $-15,000^\circ \cdot \text{cm}^2 \cdot \text{dmol}^{-1}$, which was 25% greater than that for MBP alone (8). The X-ray structure of MBP was reported to be 44.9% helical and 15.6% beta sheet (24). The greater CD signal at 222 nm due to the addition of RP2 to MBP indicated that RP2 alone contained a significant alpha-helical conformation (33), which was in good agreement with our secondary-structure prediction. Removal of zinc by the addition of EDTA only leads to a less than 10% increase in the CD signal at 222 nm. The far-UV CD spectrum of the protein in the presence of EDTA is very similar to that in the presence of zinc, suggesting that zinc binding did not lead to a major change in the secondary structure of MBP-RP2.

Fluorescence spectroscopy is very sensitive to changes in the environment of aromatic amino acid residues. Since there are several Trp residues in RP2, Trp fluorescence was used as a probe to monitor the change in the tertiary structure of RP2 caused by zinc binding. In the fluorescence spectrum studies, the emission spectrum was 300 to 400 nm and the excitation spectrum was 260 to 300 nm. When excited at 285 nm, RP2 has an emission spectrum maximum at 336 nm, which is similar to that of proteins with a well-folded tertiary structure (15). Both the maxima of the excitation and emission spectra of RP2 and the fluorescence intensity remained the same whether RP2 was renatured with Zn or EDTA (Fig. 5C), and thus, no significant changes in the tertiary structure and the environment of the aromatic residues of the fusion protein were observed in the presence or absence of Zn. Taken together, the data from both far-UV and fluorescence studies indicate that zinc binding does not play a major role in maintaining the secondary and tertiary structures of the RP2 protein.

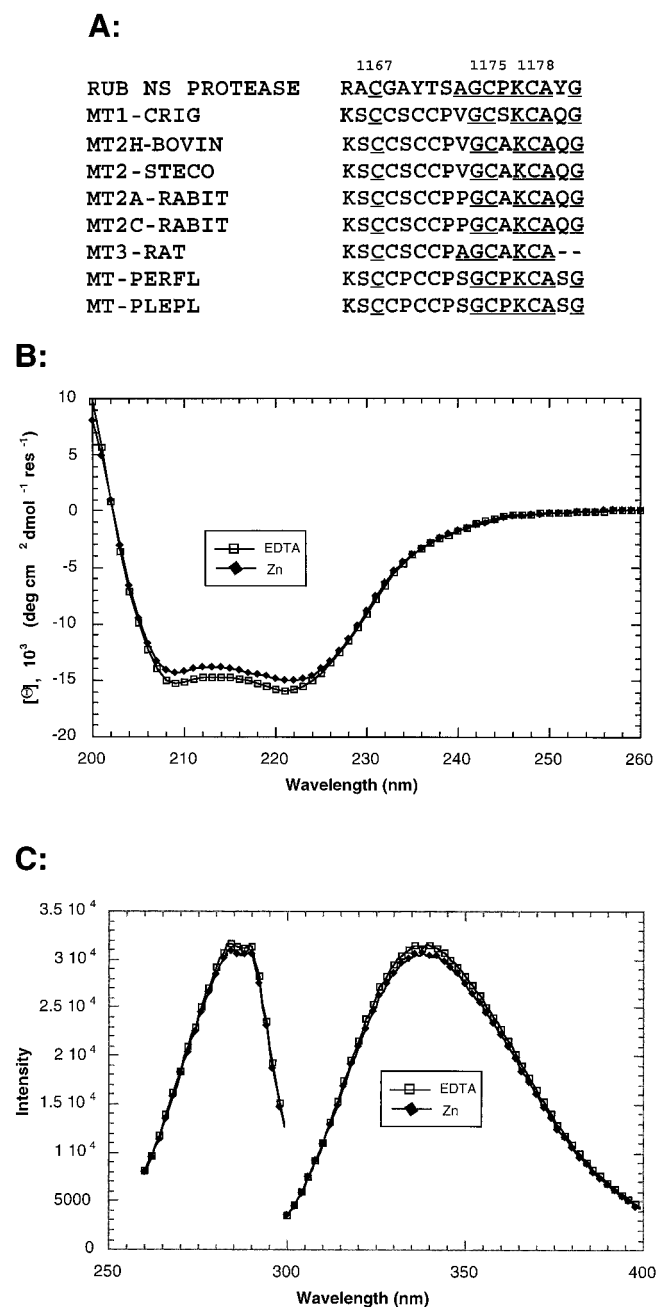


FIG. 5. Sequence alignment and conformational analyses. (A) Alignment of the primary sequence of the ZP2 Zn binding domain of the RUB NS protease (aa 1165 to 1181; Cys residues are indicated) with a Zn binding site within the C-terminal α domain of eight different types of metallothionein in the SwissProt sequence database. Alignment was done by BLAST (2). The accession numbers in the SwissProt sequence database are P02804 (MT1_CRIGR), P55943 (MT2H_BOVIN), P14425 (MT2_STECO), P18055 (MT2A_RABIT), P80290 (MT2C_RABIT), P37361 (MT3_RAT), P52725 (MT_PERFL), and P07216 (MT_PLEPL). (B) Far-UV CD spectra of 1.6 μ M NS protease fusion protein RP2 denatured and renatured in the presence of Zn (\blacklozenge) or EDTA (\square) in 20 mM Tris \cdot HCl at pH 7.4. (C) Excitation (left) and emission (right) spectra of the NS protease fusion protein RP2 denatured and renatured in the presence of Zn or EDTA in 20 mM Tris \cdot HCl at pH 7.4. The excitation wavelength for the emission spectra was 285 nm, and the emission wavelength for the excitation spectra was 336 nm. Far-UV CD and fluorescence analyses were done on at least three independent preparations of denatured-renatured RP2; representative results are shown in panels B and C.

A cleavage site mutation is lethal for RUB. Although protease cleavage of the replicase precursor is common to all of the positive-stranded RNA viruses of animals studied thus far, in only a few cases has insight into the function of this processing been gained (28, e.g.). To determine whether cleavage of the NS precursor is essential for RUB viability, a cleavage site mutation changing Gly1301 to Val was introduced into the RUB infectious clone by transferring the *RsrII-EcoRV* fragment from pTM1/nsRUB-JV (G1301 to Val) (18) to the RUB infectious cDNA clone Robo302. Two different ligations were performed, and 10 colonies were selected from each subsequent transformation and sequenced to confirm the mutation. Several constructs from each ligation were used as the templates for in vitro transcription, and Vero cells were transfected with each of these in vitro transcripts. No cytopathic effect was detected by 6 to 7 days posttransfection in cultures transfected with any of the 12 different mutant clones. With control Robo302 transcripts, a cytopathic effect was observed 3 to 4 days posttransfection. This indicates that processing of the RUB NSP ORF is necessary for virus replication and viability.

DISCUSSION

The RUB NSP ORF encodes a protease that cleaves the P200 NSP precursor at a single site to produce two products. In all of the plus-strand RNA viruses of animals thus far studied, a virus-encoded protease is present which processes the replicase precursor. In this study, a cleavage site mutation shown to be lethal to the virus and thus the cleavage is necessary for RUB replication. Although the RUB NS protease was predicted to be a PCP with a catalytic dyad of Cys1152 and His1273, we recently found that the RUB NS protease requires zinc for activity (18), at the time a novel finding among viral cellular PCPs. More recently, murine hepatitis virus (MHV) PLP-1, a PCP, was shown to bind Zn and mutagenesis of the four Cys ligands predicted to form a Zn finger was found to abrogate protease activity (11).

We approached our analysis of Zn binding by the RUB NS protease by engineering expression of the minimal NS protease domain in a bacterial system as a fusion protein. The NS protease fusion protein was functional even in the presence of the fusion domain both in bacteria and in vitro when denatured and refolded in the presence of Zn. Therefore, this work was done on an active product. Atomic absorption analysis indicated that the NS protease fusion protein bound one zinc ion when purified directly from bacteria, but when the NS protease fusion protein was denatured and refolded in the presence of Zn, the moles of Zn bound per mole of protein was 1.6 mol. Two nonoverlapping Zn binding domains were subsequently identified by Zn binding assay when individual domains of the protease were expressed. This indicates that 100% acquisition of conformation with respect to Zn binding was not achieved either in the bacteria or during refolding in vitro. In all expression studies on the NS protease thus far performed, whether by in vitro translation or expression in bacteria or eukaryotic cells, cleavage has never been observed to go to completion. This is possibly due to difficulties in acquiring 100% conformation with respect to Zn binding.

Zn binding studies using individual domains of the NS protease expressed as MBP fusions localized two Zn binding motifs. One is located at a previously predicted metal binding site beginning the sequence Cys1175-X₂-Cys1178-(ZP2), while the other is located downstream (ZP3) and near the cleavage site (Gly1301) and does not contain a classic metal binding motif but does have an abundance of Cys and His residues. Mutagenesis studies showed that Cys1175 and Cys1178 within the first

domain are essential for Zn binding. Interestingly, the amino acids around Cys1175 and Cys1178 had strong homology to a zinc binding motif in several types of metallothionein. The other two members of the predicted metal binding site (His1190 and His 1204) were not essential for Zn binding. Similarly, Cys1227 and His1273 within the second domain are essential for zinc binding. Four ligands are usually involved in Zn binding, and sulfur ligands in Cys residues are most commonly associated with Zn binding. However, Zn forms complexes with nitrogen and oxygen just as readily as with sulfur, as evidenced by zinc binding by the imidazole group of histidine and carboxyl groups of glutamic and aspartic acids (31). Not all of the His residues in the second Zn binding domain were mutagenized, and both glutamic and aspartic acid residues are present in abundance in both domains (Fig. 1); some of these residues could be the additional ligands. Water is also a common ligand and appears universally at all of the Zn catalytic sites thus far characterized (30). In this regard, it was interesting that both Cys1175 and Cys1178 were predicted at the loop region of the protein with large solvent accessibility. With respect to the other Zn-dependent viral proteases, the HRV 2A protease utilizes three Cys and one His residue as Zn binding ligands (25), the HCV NS3 protease uses three Cys residues and a water molecule (16, 26), while MHV PLP-1 is predicted to use four Cys residues (11).

All of the residues necessary for Zn binding in the two Zn binding domains are essential for protease activity. Considering the computer-based prediction that the RUB NS protease is a PCP (9), Zn binding by these domains would play a structural role in determining the conformation of the protease. A computer-generated model makes this prediction for the function of the Zn ion bound by MHV PLP-1 (11). While we have no evidence as to the function of either Zn binding domain in the RUB NS protease, based on the homology with several types of metallothionein, we propose that the first Zn binding domain is structural in nature. In addition to the Zn binding residues, several Cys residues not involved in Zn binding, including Cys1152, one proposed member of the PCP catalytic dyad, were essential for protease activity. Interestingly, the other member of the predicted PCP catalytic dyad, His1273, was essential for zinc binding, indicating that it is not an actual catalytic residue of the protease.

Considering the role of Zn binding in the structure of Zn-dependent viral proteases, as well as Zn binding proteins in general, we performed structural studies on the MBP-NS protease fusion protein denatured and refolded in vitro in the presence or absence of Zn. Neither far-UV CD nor fluorescence analysis found that the presence of Zn causes a significant change in the secondary and tertiary structures of the protein. This indicated that, at most, only a localized effect on the protein structure could be associated with Zn binding. Similar analysis of the interaction of Zn with the individual binding domains is necessary to elucidate such localized effects. Computer analysis indicated that both ends of the minimal protease domain contain a β -sheet secondary structure while the interior region (mainly ZP2) contains several stretches of α -helix segments encompassing the first Zn binding site. Far-UV CD analysis confirmed the existence of an α -helical secondary structure.

In a final attempt to gain insight into NS protease activity, a battery of protease inhibitors were employed. The cysteine protease inhibitor antipain or E-64C or -D did not inhibit protease activity, although it also failed to inhibit the SIN nsP2 protease. More stringent alkylating agents, iodoacetamide and *N*-ethylmaleimide, were also tested, but they radically altered the profile of bands on the gel (data not shown) and thus were

not useful. The failure of DTT to inhibit NS protease activity indicated that disulfide-bonded Cys residues are not essential to NS protease activity. NS protease activity was completely blocked by metal ion chelators such as 1,10-OP and EDTA but not EGTA. EDTA has strong zinc binding affinity, and its zinc binding affinity is several orders greater than that of EGTA (the $K_{d,s}$ of EGTA and EDTA for zinc are $10^{-12.9}$ and $10^{-16.4}$ M) (3). The specific inhibition by EDTA instead of EGTA indicates that RP2 might contain a zinc binding site with relatively high affinity. The activity of two other Zn-dependent viral proteases, the HRV 2A protease and MHV PLP-1, is not inhibited by the presence of chelating agents, while the activity of the HCV NS3 protease is inhibited by these agents. This suggests that Zn-dependent viral proteases have different zinc affinities.

Most interestingly, a specific metalloprotease inhibitor, captopril, which can specifically inhibit the angiotensin-converting enzyme (23), a zinc-dependent dipeptidyl carboxypeptidase with two zinc binding sites, completely inhibited the NS protease activity. Among the other metalloprotease inhibitors tested (17), phosphoramidon showed an intermediate level of inhibition while inhibition by thiorphan was minimal. With this evidence, in addition to the finding that His1273 is required for Zn binding, it is possible that the NS protease is not a PCP but rather a novel viral metalloprotease. The expression of this protease in bacteria as an active enzyme offers promise that further structural studies can be done to resolve this possibility.

ACKNOWLEDGMENTS

We thank P. C. Tai and members of his laboratory for helpful discussions and advice on fast-performance liquid chromatography and Yiming Ye for help with CD and fluorescence studies. We also thank Robert Wohlhueter for amino acid analysis.

This research was supported by a grant from the NIH (AI 21389) to T.K.F. The inductively coupled plasma mass spectrometer was purchased with funds from a NSF grant (EAR-94-05716) to A.M.G. and D. A. Vanko. X.L. was supported in part by funding from the Georgia State University Research Program Enhancement program.

REFERENCES

- Alder, M., J. D. Nicholson, and B. E. Hackley. 1998. Efficacy of a novel metalloprotease inhibitor on botulinum neurotoxin B activity. *FEBS Lett.* **429**:234–238.
- Altschul, S. F., T. L. Madden, A. A. Schaffer, J. Zhang, Z. Zhang, W. Miller, and D. J. Lipman. 1997. Gapped BLAST and PSI-BLAST: a new generation of protein database search programs. *Nucleic Acids Res.* **25**:3389–3402.
- Auld, D. S. 1988. Use of chelating agents to inhibit enzymes. *Methods Enzymol.* **158**:110–114.
- Chen, H., W. Kong, and R. Roos. 1995. The leader peptide of Theiler's murine encephalomyelitis virus is a zinc-binding protein. *J. Virol.* **69**:8076–8078.
- Chen, J., J. H. Strauss, E. G. Strauss, and T. K. Frey. 1996. Characterization of the rubella virus nonstructural protease domain and its cleavage site. *J. Virol.* **70**:4707–4713.
- Dominguez, G. 1991. Determination and analysis of the sequence of the genome RNA of rubella virus. Ph.D. dissertation, Georgia State University, Atlanta.
- Frey, T. K. 1994. Molecular biology of rubella virus. *Adv. Virus Res.* **44**:69–160.
- Ganesh, C., A. N. Shah, C. P. Swaminathan, A. Suroliya, and R. Varadarajan. 1997. Thermodynamic characterization of the reversible, two-state unfolding of maltose binding protein, a large two-domain protein. *Biochemistry* **36**:5020–5028.
- Gorbalenya, A. E., E. V. Koonin, and M. M.-C. Lai. 1991. Putative papain-related thiol protease of positive-strand RNA viruses. *FEBS Lett.* **288**:201–205.
- Gros, C., and G. Wengler. 1996. Identification of an RNA-stimulated NTPase in the predicted helicase sequence of the rubella virus nonstructural polyprotein. *Virology* **217**:367–372.
- Herold, J., S. G. Siddell, and A. E. Gorbalenya. 1999. A human RNA viral cysteine proteinase that depends upon a unique Zn²⁺-binding finger connecting the two domains of a papain-like fold. *J. Biol. Chem.* **274**:14918–14925.
- Hibbetts, K., B. Hines, and D. Williams. 1999. An overview of proteinase inhibitors. *J. Vet. Intern. Med.* **13**:302–308.
- Ho, S. N., H. D. Hunt, R. M. Horton, J. K. Pullen, and L. R. Pease. 1989. Site-directed mutagenesis by overlap extension using the polymerase chain reaction. *Gene* **77**:51–59.
- Keck, J. G., F. Feigenbaum, and B. Moss. 1993. Mutational analysis of a predicted zinc-binding motif in the 26-kilodalton protein encoded by the vaccinia virus AsL gene: correlation of zinc binding with late transcriptional transactivation activity. *J. Virol.* **67**:5749–5753.
- Khorasanizadeh, S., I. D. Peters, T. R. Butt, and H. Roder. 1993. Folding and stability of a tryptophan-containing mutant of ubiquitin. *Biochemistry* **32**:7054–7063.
- Kim, J. L., K. A. Morgenstern, C. Lin, T. Fox, M. D. Dwyer, J. A. Landro, S. P. Chambers, W. Markland, C. A. Lepre, E. T. O'Malley, S. L. Harbeson, C. Rice, M. A. Murcko, P. R. Caron, and J. A. Thomson. 1996. Crystal structure of the hepatitis C virus NS3 protease domain complexed with a synthetic NS4A cofactor peptide. *Cell* **87**:343–355.
- Krane, S. M. 1994. Clinical importance of metalloproteinases and their inhibitors. *Ann. N. Y. Acad. Sci.* **732**:1–10.
- Liu, X., S. L. Ropp, R. J. Jackson, and T. K. Frey. 1998. The rubella virus nonstructural protease requires divalent cations for activity and functions in *trans*. *J. Virol.* **72**:4463–4466.
- Marr, L. D., C.-Y. Wang, and T. K. Frey. 1994. Expression of the rubella virus nonstructural protein ORF and demonstration of proteolytic processing. *Virology* **198**:586–592.
- Pugachev, K., E. S. Abernathy, and T. K. Frey. 1997. Improvement of the specific infectivity of the rubella virus (RUB) infectious clone: determinants of cytopathogenicity induced by RUB map to the nonstructural proteins. *J. Virol.* **71**:562–568.
- Rost, B., and C. Sander. 1993. Prediction of protein secondary structure at better than 70% accuracy. *J. Mol. Biol.* **232**:584–599.
- Saavedra-Alanis, V. M., P. Rysavy, L. E. Rosengerg, and F. Kalousek. 1994. Rat liver mitochondrial processing peptidase. *J. Biol. Chem.* **269**:9284–9288.
- Shapiro, R., and J. F. Riordan. 1984. Inhibition of angiotensin converting enzyme: dependence on chloride. *Biochemistry* **23**:5234–5240.
- Sharff, A. J., L. E. Rodseth, J. C. Spurlino, and F. A. Quioco. 1992. Crystallographic evidence of a large ligand-induced hinge-twist motion between the two domains of the maltodextrin binding protein involved in active transport and chemotaxis. *Biochemistry* **31**:10657–10663.
- Sommergruber, W., J. Seipelt, F. Fessl, T. Skem, H.-D. Liebig, and G. Casari. 1997. Mutational analyses support a model for the HRV 2A proteinase. *Virology* **234**:203–214.
- Stempniak, M., Z. Hostomska, B. R. Nides, and Z. Hostomsky. 1997. The NS3 proteinase domain of hepatitis C virus is a zinc-containing enzyme. *J. Virol.* **71**:2881–2886.
- Stillman, M. J., and A. Zelazowski. 1988. Domain specificity in metal binding to metallothionein. *J. Biol. Chem.* **263**:6128–6133.
- Strauss, J. H., and E. G. Strauss. 1994. The alphaviruses: gene expression, replication, and evolution. *Microbiol. Rev.* **58**:491–562.
- Sytkowski, A. J., and B. L. Vallee. 1979. Cadmium-109 as a probe of the metal binding sites in horse liver alcohol dehydrogenase. *Biochemistry* **18**:4095–4099.
- Vallee, B. L., and D. S. Auld. 1989. Active-site zinc ligands and activated H₂O of zinc enzymes. *Proc. Natl. Acad. Sci. USA* **87**:220–224.
- Vallee, B. L., and D. S. Auld. 1990. Zinc coordination, function, and structure of zinc enzymes and other proteins. *Biochemistry* **29**:5647–5659.
- Voss, T., R. Meyer, and W. Sommergruber. 1995. Spectroscopic characterization of rhinoviral protease 2A: Zn is essential for the structural integrity. *Protein Sci.* **4**:2526–2531.
- Yang, J., M. Buck, M. Pitkeathly, M. Kotik, D. Haynie, C. Dobson, and S. Radford. 1995. Conformational properties of four peptides spanning the sequence of hen lysozyme. *J. Mol. Biol.* **252**:483–491.